Materials Science and Engineering C 60 (2016) 239–245

Contents lists available at ScienceDirect

Materials Science and Engineering C

journal homepage: www.elsevier.com/locate/msec

Disinfection of titanium dioxide nanotubes using super-oxidized water decrease bacterial viability without disrupting osteoblast behavior

Ernesto Beltrán-Partida [a,b], Benjamín Valdez-Salas [b,*], Alan Escamilla [b], Mario Curiel [b], Ernesto Valdez-Salas [c], Nicola Nedev [b], Jose M. Bastidas [d]

[a] Department of Biomaterials, Dental Materials and Tissue Engineering, Faculty of Dentistry Mexicali, Autonomous University of Baja California, Av. Zotoluca and Chinampas St., 21040 Mexicali, Baja California, Mexico
[b] Department of Corrosion and Materials, Engineering Institute, Autonomous University of Baja California, Blvd. Benito Juarez and Normal St., 21280 Mexicali, Baja California, Mexico
[c] Ixchel Medical Centre, Av. Bravo y Obregón, 21000 Mexicali, Baja California, Mexico
[d] National Centre for Metallurgical Research, CSIC, Av. Gregorio del Amo 8, 28040 Madrid, Spain

ARTICLE INFO

Article history:
Received 8 May 2015
Received in revised form 20 October 2015
Accepted 16 November 2015
Available online 17 November 2015

Keywords:
Titanium
Nanostructures
Sterilization
Bacterial viability
Super-oxidized water

ABSTRACT

Amorphous titanium dioxide (TiO_2) nanotubes (NTs) on Ti6Al4V alloy were synthesized by anodization using a commercially available super-oxidized water (SOW). The NT surfaces were sterilized by ultraviolet (UV) irradiation and disinfected using SOW. The adhesion and cellular morphology of pig periosteal osteoblast (PPO) cells and the behavior of *Staphylococcus aureus* (*S. aureus*) cultured on the sterilized and disinfected surfaces were investigated. A non-anodized Ti6Al4V disc sterilized by UV irradiation (without SOW) was used as control. The results of this study reveal that the adhesion, morphology and filopodia development of PPO cells in NTs are dramatically improved, suggesting that SOW cleaning may not disrupt the benefits obtained by NTs. Significantly decreased bacterial viability in NTs after cleaning with SOW and comparing with non-cleaned NTs was seen. The results suggest that UV and SOW could be a recommendable method for implant sterilization and disinfection without altering osteoblast behavior while decreasing bacterial viability.

1. Introduction

Titanium (Ti) and Ti-based alloys are among the most widely used clinical materials for orthopedic and dental implants [1], due to their mechanical strength, light weight, corrosion resistance by the formation of a protective TiO_2 layer, and biocompatibility [1,2]. However, bacterial adhesion on the implant surface is a complication that can critically affect the success of biomaterials due to the ability of bacteria to form biofilms which lead to implant failure [3–5]. To address these problems, this study considers NTs produced by anodization, as they can be synthesized with controlled order, improved corrosion resistance, increased surface roughness, a lower water contact angle, and excellent biocompatibility compared to non-modified Ti surfaces [2,6,7]. It has also been suggested that a 70–100 nm NT diameter promotes alkaline phosphatase activity levels and increased calcium deposition compared to non-anodized Ti and smaller NT diameters [8], information that propose 80 nm NTs as a bone forming-functional coating. On the other hand, Ercan et al., reported decreased *Staphylococcus aureus* viability on amorphous 80 nm NTs after comparing to minor diameter NTs (20, 40 and 60 nm) and non-anodized Ti [9]. Likewise, Arenas et al., described that amorphous 100 nm NTs built on Ti6Al4V by anodization promotes superior antibacterial effects against *S. aureus* after comparing to non-anodized Ti6Al4V [10]. As well, they suggested a reduced colonization rate of a clinically *S. aureus* strain (isolated from an infected hip prosthesis) cultured on NT surfaces after comparing to 20 nm diameter TiO_2 nanopores and non-anodized Ti6Al4V [10]. Moreover, in a recent study we observed an elevated and sustained antibacterial performance against *S. aureus* for up to 5 days on amorphous 80 nm NTs fabricated on Ti6Al4V using SOW for anodization, but not for surface disinfection [11]. This information advocates the use of 80–100 nm NTs as an appropriate antibacterial nanostructured coating.

Sterilization is defined as a process that completely eradicates or destroys bacterial life, being widely performed by physical or chemical processes [12], and has been reported to play an important role in the biological behavior (e.g. cellular adhesion or bacterial viability) of implant surfaces [2,13–15], especially Ti. In recent studies autoclaving has commonly been used as a sterilizing technique for Ti surfaces [2], but autoclaving has shown that is capable to reduced hydrophilicity of Ti surfaces through the deposition of hydrophobic contaminants on the material surface [13], resulting in reduced cytocompatibility. Furthermore, sterilization by autoclaving has led to significantly decreased MG63 human osteoblast and MC3T3-E1 mouse osteoblast responses on NTs and non-anodized Ti [13,16]. Moreover, Kummer et al.,

* Corresponding author.
E-mail address: benval@uabc.edu.mx (B. Valdez-Salas).

http://dx.doi.org/10.1016/j.msec.2015.11.042
0928-4931/

suggested increased *S. aureus* growth on 80 and 20 nm diameter NTs and on non-anodized Ti surfaces sterilized by autoclaving, compared to ethanol and UV sterilization methods [2].

SOW is an electrolyzed water that contains oxidizing species such as H_2O_2, oxidizing radical (i.e. hypochlorous species) an chlorine molecules like hypochlorite [17,18]. It has been widely used as a disinfectant for medical instruments and inanimate surfaces [17]. Furthermore, it has been reported to be effective in the treatment of infectious diseases such as skin defects or ulcers, peritonitis and intraperitoneal abscesses [17,19], suggesting that SOW acts as a potent antibacterial agent with a broad-spectrum antibacterial efficacy [20]. In this manner, it has been proposed that SOW works destroying the covalent bonds of the nucleic acid chains, as well as the protein chains in *Escherichia coli* (*E. coli*) JM109 [21,22]. Moreover, an AFM study showed that SOW in contact with *E. coli* for 30 s was able to induced cellular swelling and at the end of 5 min of exposure it was observed that the cells were completely destroyed [23]. These data suggested that SOW acts as an antibacterial agent that negatively interferes with the metabolic activity and membrane integrity of bacteria. On the other hand, SOW has also been recommended for handwashing by medical personnel [17], being proposed as a non-cytotoxic substance. However, the promising effects of SOW as a disinfectant agent have not been investigated on nanostructured Ti. On the basis of the above it is hypothesized that Ti6Al4V NT surfaces sterilized with UV and disinfected by SOW rinsing will offer lower bacterial viability without altering osteoblast adhesion and morphology.

The present study evaluates for the first time the bacterial behavior of 80 nm TiO_2 NTs on Ti6Al4V alloy sterilized by UV and disinfected using a commercially available super-oxidized solution. Osteoblast behavior is explored by evaluating cell adhesion, cellular morphology and the formation of filopodias, as well as cytoplasmic stress fibers. The surface morphology of the material was analyzed by field emission scanning electron microscopy (FE-SEM), the chemical composition by energy dispersive X-ray spectroscopy (EDX), and the surface roughness by atomic force microscopy (AFM). *S. aureus* viability on the surfaces was assessed by colony-forming unit (CFU) calculation and bacteria morphology was analyzed using scanning electron microscopy (SEM). Osteoblast behavior was also examined by SEM and fluorescence microscopy.

2. Materials and methods

2.1. Synthesis of NTs

NTs were synthetized as described in a previous study [24]. Discs of Ti6Al4V (ASTM F-136; Supra Alloys Inc., Camarillo, CA, USA) with 150 mm diameter and 5 mm thickness were polished using SiC emery paper (100 to 2000 grit) and 1-μm alumina to achieve a mirror finish. The discs were then mounted on a special flat 125 mL cell and electrolytically anodized using Microdacyn 60® super-oxidized water (Oculus Technologies, Guadalajara, JAL, MEX) at pH 6.8, containing 10 mg/L of NH_4F (Sigma-Aldrich, USA) and 100 mg/L NaCl (Sigma-Aldrich, USA). A 20 V potential was applied using a DC power supply for 5 min and a platinum mesh as counter electrode. The process was carried out at room temperature (defined here as RT). Finally, the discs were cleaned in an ultrasonic bath with distilled water for 5 min to eliminate residues of fluoride salts [25], rinsed with isopropyl alcohol, and dried in a desiccator for 12 h. All experimental substrates were sterilized by UV irradiation (285 nm UVB light source) for 30 min on each side [2,13].In order to systematically evaluate the effect of SOW rinsing, an anodized-Ti6Al4V NTs and non-anodized Ti6Al4V materials (namely here as NT-SOW and Ti6Al4V-SOW respectively) were disinfected by immersion in 20 mL of SOW for 1 h and finally dried at RT before use. A non-anodized Ti6Al4V alloy disc (denoted here as Ti6Al4V) was used as control. Finally, an anodized-Ti6Al4V NT (NT) surface was used as a negative control.

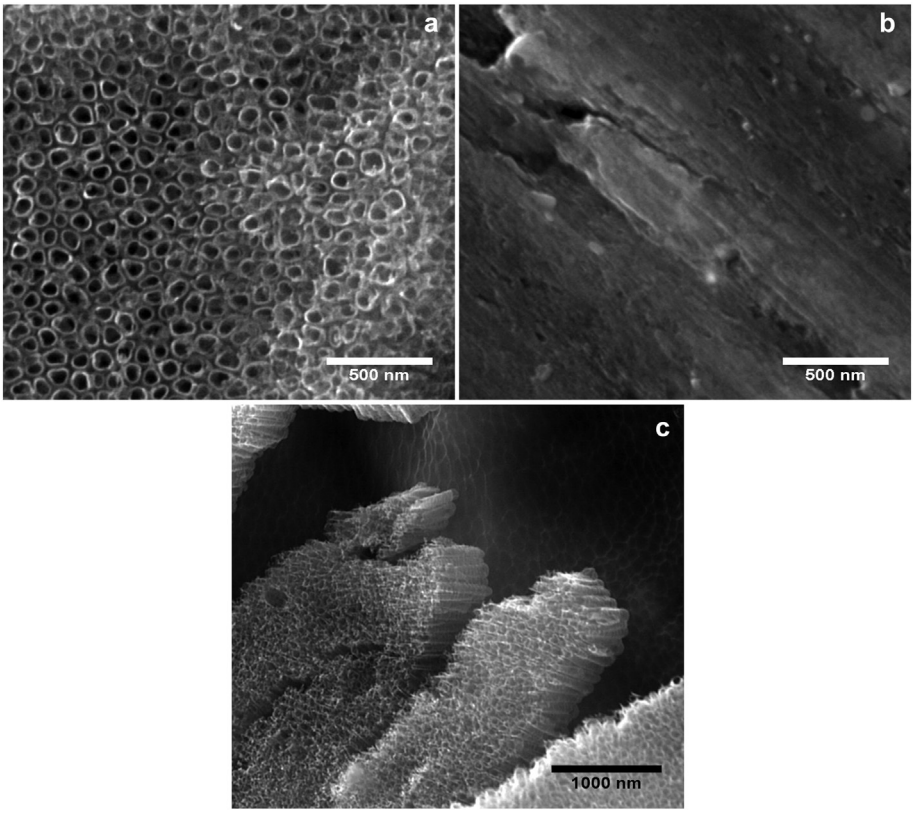

Fig. 1. FE-SEM micrographs of the experimental surfaces cleaned by SOW: (a) anodized Ti6Al4V alloy illustrating the presence of NTs. (b) Ti6Al4V surface showing a flat surface. (c) A cross-section view of NTs.

Table 1
Elemental composition percentages of the experimental surfaces.

Sample	C (%)	V (%)	Al (%)	Ti (%)	O (%)	F (%)
Anodized NT-SOW	4.61	—	4.06	68.10	20.32	2.91
Anodized NTs	5.19	—	4.80	61.50	24.00	4.51
Ti6Al4V-SOW	0.97	4.11	6.26	88.66	—	—
Ti6Al4V	3.40	3.43	6.06	87.11	—	—

2.2. Surface characterization

The structural morphology of the sample surfaces were characterized by FE-SEM (Tescan LYRA 3, Brno Czech Republic), taking images at a 20 kV accelerating voltage. The chemical composition of the alloy surface was assessed by EDX (Tescan LYRA 3, Brno Czech Republic) using a silicon drift detector coupled to the FE-SEM.

An AFM (Quesant Q-Scope 350, AMBIOS, Agura Hills, CA, USA) was used to measure the surface roughness of the experimental substrates. The process was performed at RT using an anti-acoustic box to prevent noise, which can affect the measurements. Topographic images were obtained operating at a scan rate of 1 Hz. A 40-μm X–Y and 4-μm Z scanner equipped with silicon tips and 10 nm tip curvature was used. The experiment scan surface area was 1 μm^2. The root mean square (RMS) is provided in order to quantitatively compare the roughness between NTs and Ti6Al4V surfaces.

2.3. Osteoblast culture and characterization on the materials

For these studies, PPO cells were isolated from pig femur periosteal bone [24]. The cells were cultured in DMEM (Dulbecco's Modified Eagle's Medium/Ham's F-12, Invitrogen, Carlsbad, CA, USA) supplemented with 10% fetal bovine serum (FBS; Invitrogen, Carlsbad, CA, USA) and a volume fraction of 1% penicillin–streptomycin (PS; Invitrogen, Carlsbad, CA, USA) at 37 °C in 5% CO_2. Each experimental sample (NT-SOW, NTs, Ti6Al4V-SOW and Ti6Al4V control surface) was placed in an individual well of a 12-well polystyrene plate. The cells were seeded using 1 mL of medium containing a concentration of 2×10^4 cells per mL onto the materials and stored in a CO_2 chamber for the experimental time [8,24].

In order to count adhered osteoblasts on the experimental samples, DAPI staining was performed. At 4, 12 and 24 h after culturing, the cells on the substrates were washed three times in phosphate-buffered saline (1× PBS) solution to remove non-adhered cells. The remaining cells were fixed in 4% paraformaldehyde (indicated here as PA) in 1× PBS for 30 min at RT. Once fixed, the cells were stained with 4′,6′-diamidino-2-phenylindole (DAPI; Molecular Probes, Carlsbad, CA, USA) in 1× PBS and incubated for 5 min at RT, and then washed three times with 1× PBS [26]. Finally, the samples were inverted onto coverslips with a fluorescence mounting medium (DAKO, Agilent Technologies, Carpinteria, CA, USA), visualized, photographed and counted in five random fields using a blue filter by a fluorescence microscope (Axio Observer A1, Carl Zeiss, Thornwood, NY, USA).

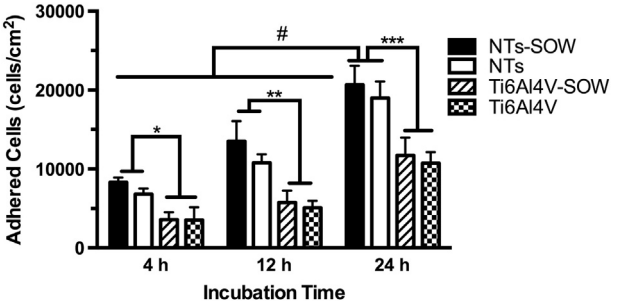

Fig. 3. Number of adhered PPO cells on the biomaterial surfaces as a function of time. Values are mean ± SD, N = 3. *, ** and *** denote differences between NT-SOW and NT groups versus Ti6Al4V-SOW and Ti6Al4V control surfaces after 4 h, 12 h and 24 h of incubation respectively. # indicates significant differences for NT-SOW and NT substrates at 24 h after comparing to all the experimental materials cultured at 4 h and 12 h.

In contemplation to analyze the formation of cellular stress fibers on the disinfected materials, cytoskeletal actin immunofluorescence was performed after 24 h of culture on the NT-SOW and Ti6Al4V-SOW substrates. The samples were initially washed three times with 1× PBS and fixed with PA for 30 min at RT. Once fixed, they were again washed three times with 1× PBS. To permeabilize the cells, 0.1% Triton X-100 in 1× PBS solution was added for 20 min. The cells were washed three times with 1× PBS and the samples were incubated for 1 h at RT in bovine serum albumin (BSA) blocking solution (1% BSA/1× PBS) and washed with 1× PBS. Next, the cells were incubated with Alexa Fluor 488 phalloidin (1:100; Invitrogen, USA) in blocking solution and incubated for 1 h. The cells were again washed three times and counterstained with DAPI for 10 min at RT. Finally the specimens were inverted onto coverslips with a fluorescence mounting medium, examined and photographed using a green (actin) and blue (DAPI) filter by means of a fluorescence microscope [27].

To characterize cell morphology a SEM (JSM-6010LA, JEOL, Tokyo, Japan) analysis was carried out as described by others [8,24]. After

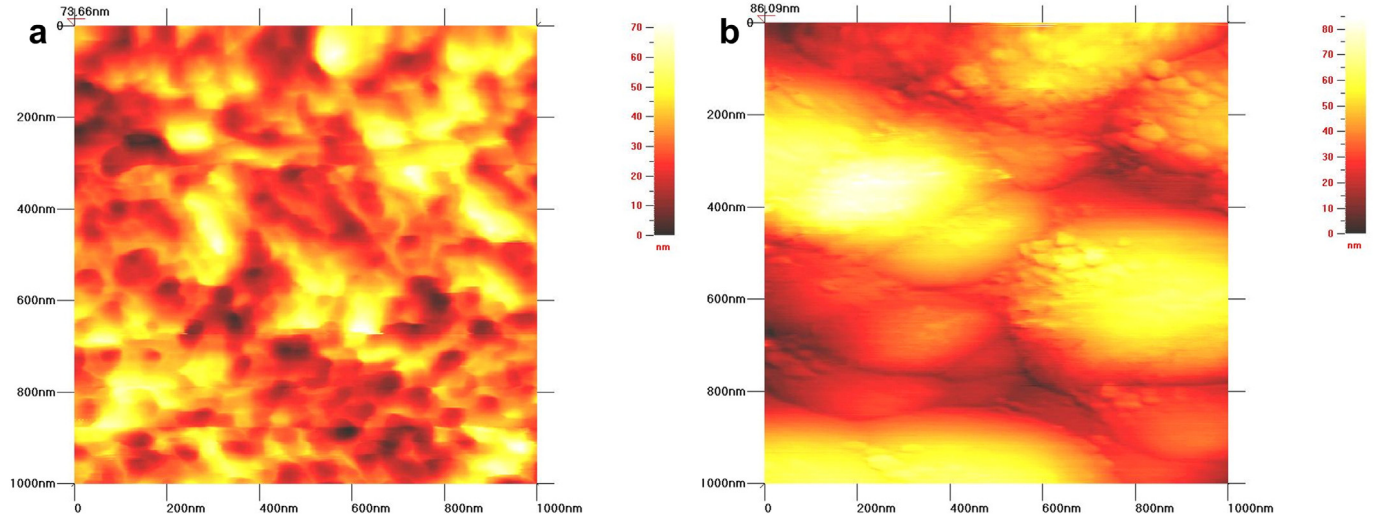

Fig. 2. AFM micrographs of the disinfected Ti6Al4V surfaces: (a) Ti6Al4V surface with anodized NTs showing a rougher surface. (b) Ti6Al4V surface representing a smooth and flat surface.

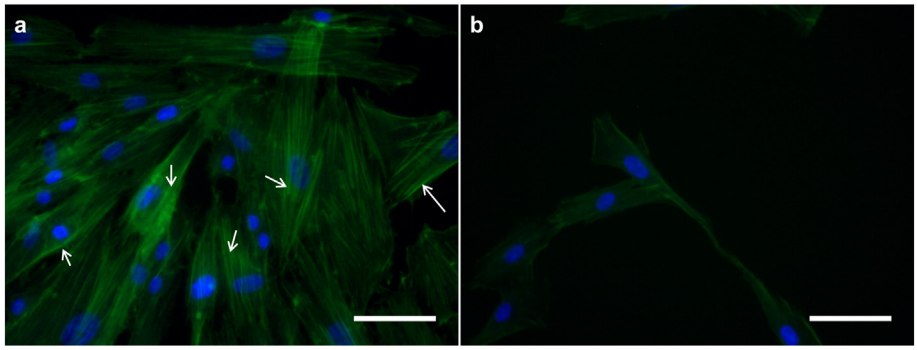

Fig. 4. Fluorescence detection of F-actin in PPO cells cultured on the disinfected experimental materials for 24 h: (a) NT-SOW illustrating spreaded cells with and organized and aligned cytoskeleton, with the evident presence of cytoplasm stress fibers (pointed arrows). (b) Ti6Al4V-SOW surface showing an elongated cellular morphology without the presence of cytoplasm stress fibers. Scale bars are 50 μm.

24 h of seeding, cells on the experimental specimens (NT-SOW and Ti6Al4V-SOW) were washed twice with 1× PBS and fixed with 5% *w/v* glutaraldehyde (Sigma-Aldrich, St. Louis, MO, USA) in PBS for 2 h. After fixation they were washed three times with 1× PBS (10 min each). The cells were then dehydrated in grade series of ethanol (50, 70, 90 and 100%) for 30 min at each concentration. Finally, the samples were sputter-coated with gold (10 nm gold layer) for 8 s. The morphology of the adhered osteoblasts was observed using a SEM at 5 kV accelerating voltage.

2.4. Bacterial culture and characterization

For bacterial growth experiments, *S. aureus* (Strain American Type Cell Culture Collection 25923, American Type Culture Collection, Manassas, VA, USA) was used. For the preparation of the inoculums, the strain was freshly grown overnight on tryptic soy agar (TSA) plates (Beckton Dickinson, Sparks, Maryland, USA). Discrete colonies were obtained from TSA plates and suspended in tryptic soy broth (TSB) to an optical density (O.D.) of 0.3, pH 7.0; assessed using a spectrophotometer (LAMBDA 25, Perkin Elmer, Connecticut, USA).

For the determination of viable cells on the samples, 100 μL of *S. aureus* suspension containing approximately 1×10^7 CFU/mL (O.D. 0.3) plus 100 μL of fresh TSB was used to cover the surface of the material. This inoculum was incubated on the specimens for 4 and 24 h at 37 °C in a static model. After the corresponding incubation times, the specimens were rinsed twice with 1× PBS to remove any unbounded cells. The substrates were transferred into sterile conical tubes (Falcon, BD Biosciences, Franklin Lakes, NJ, USA) with 5 mL of fresh TSB medium. The tubes were placed in an ultrasonic bath and sonicated for 15 min at 120 W to release the attached cells from the biomaterial. This process has been reported in previous studies to completely remove adhered cells [28,29]. The materials were then removed and the remaining suspensions were diluted with 1× PBS and cultured at 37 °C for 24 h in TSA plates. Bacterial viability was assessed by CFU counting on TSA plates. The above procedure was performed 20 times for each material [29].

In order to determine the bacterial density and morphology after 24 h of incubation, the disinfected samples were prepared for SEM analysis according to the following procedure; the discs were rinsed in 1× PBS to wash away non-adhered bacteria and then fixed with 2.5% glutaraldehyde for 2 h at 25 °C. Next, the samples were washed three times with 1× PBS (10 min each wash), dehydrated in a graded series

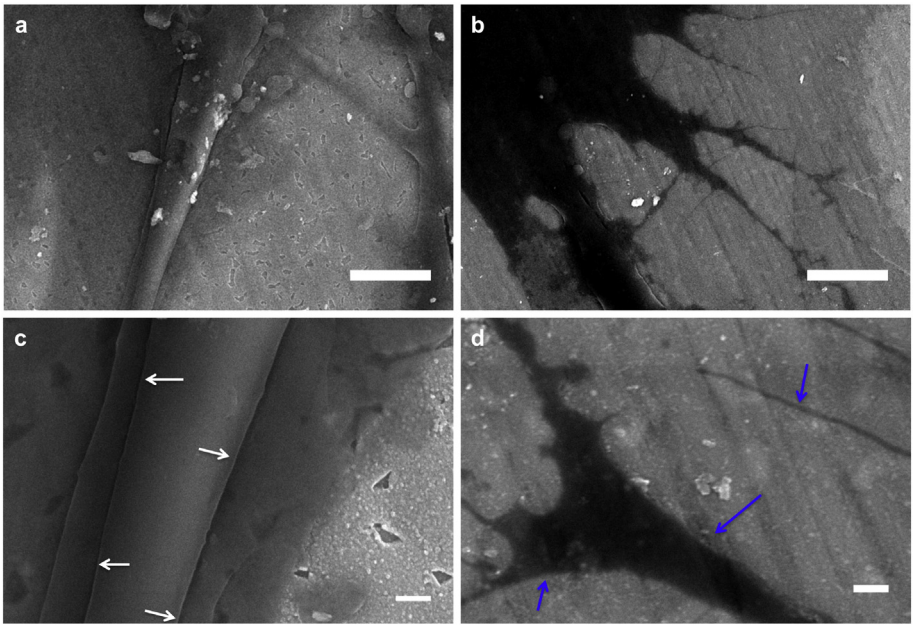

Fig. 5. SEM micrographs of osteoblasts on Ti6Al4V-SOW and NT-SOW at 24 h of culture. (a) NT-SOW surface illustrating an elongated and pronounced filopodia adhered on the substrate. (b) Ti6Al4V-SOW showing lower spreaded filopodias. (c) Higher magnification denoting a thicker filopodia anchored to the NT-SOW (white arrows) and the deposition of ECM. (d) High magnification of Ti6Al4V-SOW surface indicating a translucent adhered filopodia (blue arrows). Scale bars for a and b are 10 μm, for c and d are 1 μm. (For interpretation of the references to color in this figure legend, the reader is referred to the web version of this article.)

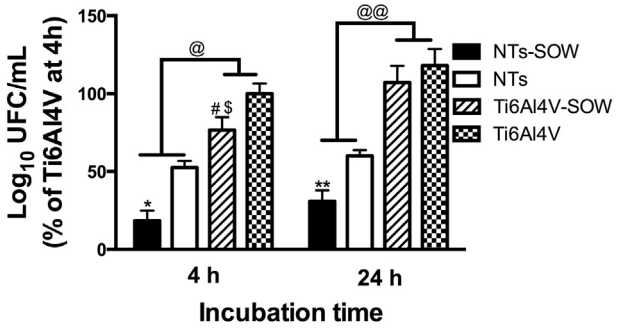

Fig. 6. Viability evaluation of *S. aureus* cultured on the surface specimens after 4 and 24 h of incubation: The bar graphs show the mean ± SD error bars, N = 3, * and ** illustrate significance between NT-SOW and NTs at 4 h and 24 h respectively. @ and @@ denote significance between NT-SOW and NT group surfaces when comparing them to Ti6Al4V-SOW and Ti6Al4V after 4 h and 24 h of culture respectively. Next, # indicates statistical difference between Ti6Al4V-SOW and Ti6Al4V control surface at 4 h of bacterial growth. Finally, $ expresses divergence among Ti6Al4V-SOW at 4 h and Ti6Al4V at 24 h of colonization.

of ethanol solutions (50, 60, 70, 80, 90 and 100% *v*/*v*), and finally sputter-coated with 10-nm gold for the analysis.

2.5. Statistical analysis

At least three independent experiments were performed, each in triplicate. For the microscopic analysis, at least five random fields were analyzed for each experimental group. Numerical data were analyzed using GraphPad Prism 6 (GraphPad Software Inc., La Jolla, CA, USA). The significance of differences between group means was determined using two-tailed unpaired Student's *t*-test or one-way ANOVA followed by Tukey's multiple comparisons test when appropriate. A $P < 0.05$ was considered statistically significant.

3. Results and discussion

The surface morphologies of the experimental materials are presented in Fig. 1. Interestingly, Fig. 1a shows FE-SEM micrographs of the anodized NTs, indicating the presence of a nanotubular and uniformly distributed layer over the alloy surface as previously reported [24]. In contrast, Fig. 1b suggests a smooth and flat surface with no evidence of nanostructured morphology, as expected [30]. Fig. 1c offers a cross-section view of the NTs. The NT diameter was estimated to be 80 nm and the length 400 nm.

The chemical composition of the material surfaces is compared in Table 1. The difference between the experimental samples consists of an increased oxygen content (24%) on the NTs and NT-SOW (20.3%) surface and the presence of trace amounts of fluoride (4.51 and 2.91%, respectively) due to anodization, information that strongly suggests the formation of a thick nanostructured layer which is not present on the Ti6Al4V-SOW and Ti6Al4V control surface, in agreement with other studies [24,25,31,32]. Indeed, this information advocates that SOW rinsing may not negatively disturb the chemical properties of the nanostructured surface.

Surface roughness represents an important parameter in the biological behavior of nanostructured surfaces [33]. Interestingly, it has been widely reported that rougher surfaces may potentially increase cellular adhesion while promoting osteoblast functionality, so attention has been paid to the surface topography of the experimental materials (Fig. 2). Fig. 2a indicates an increased surface roughness (9.19 ± 0.22 nm) on anodized NTs, as denoted by the increased formation of highly ordered nanostructured dots, data which correlates with the nanotubular morphology illustrated by FE-SEM images (Fig. 1a). The Ti6Al4V control surface topography is presented in Fig. 2b, indicating a flat and smooth surface (3.71 ± 0.68 nm) as expected, results that are in concordance with the nanotextured and flat surfaces reported in the literature [2,24,25,31,32].

Fig. 3 depicts the cell adhesion process of the PPO cells stained with DAPI on the experimental materials. The cellular adhesion process on the NT and NT-SOW surface increases dramatically with each incubation time (4 h, 12 h and 24 h) compared to the Ti6Al4V-SOW and Ti6Al4V control surface groups. Moreover, a cellular proliferation trend over the NT-SOW and NT surface could be elicited after analyzing with ANOVA (at each culture time), as a similar tendency was denoted on the Ti6Al4V-SOW and Ti6Al4V control surface, though with improved differences on the NT-SOW surface, suggesting that SOW disinfection may not disrupt the osteoblast adhesion process [7,8,31]. Interestingly, increased adhesion and proliferation of primary pig osteoblast cultured on anodized NT surfaces sterilized with UV was evidenced in a previous study [24]. Similarly, Zhao et al. suggested increased primary rat osteoblast adhesion and proliferation on anodized NTs sterilized with UV and ethanol versus an autoclaving process and polished Ti [13]. This trend was explained by the author as being due to the formation of abundant Ti–OH functional groups [34] and the removal of surface hydrophobic contaminants, especially hydrocarbons, by the UV irradiation [34,35]. They also reported increased surface energy for NTs and polished Ti surfaces sterilized by means of UV and ethanol, whereas the autoclaving process did not influence the surface energy [13]. This finding is in agreement with a recent study that described increased surface energy and MG63 osteoblast adhesion on Mg and MgCa alloys sterilized by means of ethanol immersion [12]. According to the aforementioned reports, our results suggest a similar trend to these previously reported, but more studies regarding the chemical behavior of the nanostructured surface after SOW disinfection as well as comparison with different sterilization techniques will be required in order to elucidate these trends.

Cytoskeletal actin organization and cell morphology were also analyzed by means of fluorescence microscopy, showing remarkable differences between the disinfected substrates, as depicted in Fig. 4. Initially, PPO cells cultured on the NT-SOW surfaces (Fig. 4a) showed an

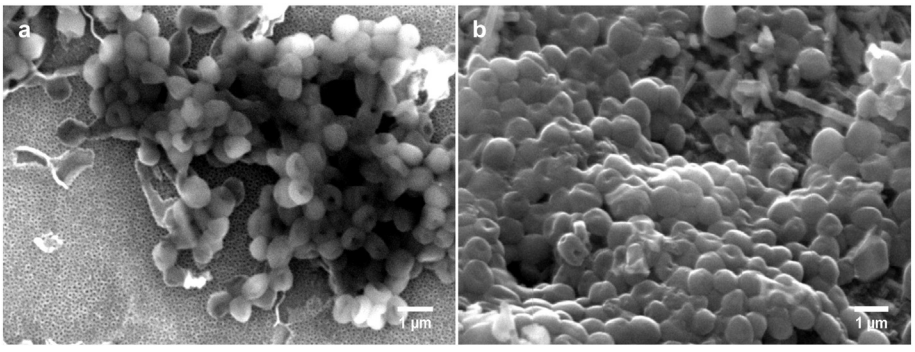

Fig. 7. SEM micrographs of adhered bacteria on the SOW-treated surfaces at 24 h of incubation: (a) Bacteria observed on the NT-SOW surface, illustrating a spherical morphology. (b) Bacteria adhered on the Ti6Al4V-SOW substrate, showing an evident biofilm formation. Denoted similar cell morphology on both experimental substrates.

organized and aligned actin assembly as well as an increased arrangement of criss-cross pattern stress fibers within the cell body (pointed arrows); trends that are in agreement with previous results regarding the configuration of osteoblast cells cultured on nanostructured titanium surfaces [27,36]. These patterns have been closely associated to an increased expression of extracellular proteins such as fibronectin and vinculin present in osteoblasts cultured on nanostructured surfaces, as well as the increased surface roughness provided by NTs (see Fig. 2), data that may explain the aligned and ordered cellular morphology and the increased formation of stress fibers observed on our NT surfaces [27,36,37]. The development of stress fibers is intimately associated to cellular movement such as cell locomotion, organelle movements and changes in cell shape [36]. Interestingly, the increased formation of stress fibers has been closely associated to osteogenesis and hydroxyapatite biomineralization processes [27,38], suggesting that SOW disinfection may not disrupt long-term osteoblast maturation on NT surfaces. When comparing the aforementioned trends with the Ti6Al4V-SOW (Fig. 4b), we detected increased cellular elongation and reduced stress fiber formations, which may suggest poorer cellular adhesion, supporting the cellular adhesion results that were previously discussed (see Fig. 3). Moreover, after comparing the SOW and control groups, we did not find significant differences, information that supports the above discussed finds.

It has been reported that cellular migration is closely associated to two cytoplasmic protrusions, lamellipodia and filopodia [39]. Filopodia is widely known to play an important role in cellular adhesion. Thus, in order to elucidate filopodia development on the SOW-treated experimental surfaces, SEM analysis was performed (Fig. 5). After 24 h, cells cultured on the NT-SOW surfaces elicited an elongated filopodia (Fig. 5a), compared to a smaller and thinner filopodia observed on the Ti6Al4V-SOW surface (Fig. 5b). Higher magnification of the cells confirmed the formation of a thicker anchored filopodia (white arrows) and increased ECM deposition around filopodia on the NT-SOW as depicted in Fig. 5c. Osteoblast filopodia anchored to NT surfaces has been associated with increased alkaline phosphatase activity and a greater secretion of Ca and P [7,8,27], which may suggest that thicker filopodia could promote improved functionality and thus that SOW disinfection may not disturb bone maturation. Furthermore, this information supports the increased stress fiber developed within the osteoblasts cultured on the NT surfaces as described above (see Fig. 4). The Ti6Al4V-SOW surface presented a thinner and translucent filopodia (blue arrows) without evident deposition of ECM as illustrated in Fig. 5d. Likewise, after comparing SOW and control surfaces we did not detect substantial differences among them, information that correlates the F-actin results.

It has been widely reported that the first hours after biomaterial implantation are crucial due to the risk of bacterial contamination on the implant surface by biofilm formation [3,4]. Therefore, *S. aureus* viability on the samples was analyzed and is shown in Fig. 6. At 4 h of bacterial culture, the NT-SOW and NT surfaces illustrated an 81.46% and 47.5% ($P < 0.05$) decrease in viable bacteria compared to the Ti6Al4V control surface. Furthermore, the NT-SOW displayed 64.7% ($P < 0.05$) reduction in healthy bacteria when correlating to the NT surface at 4 h of incubation. After 24 h the NT-SOW and NT surfaces continued to show lower bacterial viability (69 and 40% respectively) in comparison to the Ti6Al4V control surface cultured for 4 h and a similar tendency was observed for Ti6Al4V-SOW at 4 h. Likewise, a significant difference was appreciated after measuring NT-SOW and NTs versus Ti6Al4V-SOW and Ti6Al4V at 24 h of bacterial colonization. An increased bacterial number was observed between the NT-SOW and NT surfaces after 4 h and 24 h of culture, but these differences were not statistically different. In fact, a higher number of live bacteria were determined after analyzing the Ti6Al4V-SOW and Ti6Al4V control surfaces at 4 and 24 h of incubation compared to the NT-SOW and NT materials at 4 h and 24 h. After 24 h of incubation an increased number of viable bacteria i.e. 18% was calculated on the Ti6Al4V control surface compared to the same one at 4 h. In summary, a smaller number of live bacteria is observed on the NTs disinfected by SOW rinsing, while the Ti6Al4V control surface as well as Ti6Al4V-SOW yielded bacterial growth. These trends could be explained by the chemical modification of the surface due to the presence of fluoride on the NT surface after anodization. Anodization was carried out by immersion in NH_4F and the application of voltage on Ti, resulting in a greatly increased fluorine content on the anodized surfaces, basically due to the presence of TiF_6^{2-} species [9]. Moreover, the aforementioned trends are in concordance to Ercan et al., who reported a high number of dead S. aureus after 1 h of incubation on nanotubular TiO_2 [9]. Furthermore, Arenas et al. described increased antibacterial properties of anodized NTs with a high percentage of fluoride against clinical strains of *S. aureus* and *Staphylococcus epidermidis* (*S. epidermidis*) compared to conventional non-modified Ti and NTs with a lower fluoride content [5], data that are in agreement with the decreased bacterial viability reported here. The sterilization process may also count as another variable to explain the abovementioned results. For instance, Puckett et al. suggested an increased percentage of *S. aureus*, *S. epidermidis* and *Pseudomona aeroginosa* (*P. aeroginosa*) on nanotubular Ti manufactured by anodization using fluoride and autoclaving as sterilization [40]. In contrast, Lin et al. reported decreased *S. aureus* viability in vitro and in vivo on anodized 80 nm diameter NTs and on NTs loaded with gentamicin manufactured using fluoride and sterilized with UV in comparison to a conventional non-anodized Ti surface [41]. Similarly, Zhang et al. suggested decreased viability of *S. aureus* in vitro and in vivo on sintered nanotubular Ti with no presence of fluoride and NTs loaded with vancomycin but sterilized using ethylene oxide [42]. Additionally, the presence of SOW species used for NT preparation as well for surface cleaning on the nanostructured material may synergistically contributed to the increased antibacterial effects observed on NT-SOW, possibly due to the alteration of bacterial DNA and by the destruction of bacterial membrane [21,43]. In the present study, decreased viable bacteria has been elucidated on NT surfaces sterilized by means of UV and disinfected using SOW, following a similar tendency as reported by others [2,14,41]. These results may suggest the combination of UV and SOW as a novel protocol for sterilization and disinfection of nanostructured Ti surfaces.

Finally, Fig. 7 showed the *S. aureus* morphology on the experimental materials (NT-SOW and Ti6Al4V-SOW) incubated for 24 h. In Fig. 7a the presence of *S. aureus* is detected on the NT surface, denoting a spherical morphology. Similarly, Fig. 7b illustrates the presence of *S. aureus* on Ti6Al4V-SOW, indicating a similar spherical morphology. However, a high number of adhered bacteria were observed on the Ti6Al4V-SOW, supporting the bacterial viability information. These results are in concordance with Ercan et al., who reported a similar *S. aureus* morphology on anodized NT and Ti6Al4V surfaces [32]. Additionally, no significant differences on bacterial morphology were detected between the control and disinfected surfaces, data that suggest that SOW may act inhibiting *S. aureus* adhesion.

To the best of our knowledge this is the first study regarding the use of UV and SOW for Ti sterilization and disinfection. Nonetheless, we recommend the evaluation of more NT diameters, and the comparison of different sterilization techniques. Furthermore, the chemical composition of the NTs after SOW disinfection should be assessed using different analytical methods in order to elucidate more precisely the mechanisms involved in the aforementioned results. Further studies focused on in vivo behavior are recommended.

4. Conclusions

SOW has been widely used for cleaning and disinfecting medical instrumentation. This study has shown reduced bacterial viability for NTs sterilized and disinfected by means of UV and SOW without disrupting osteoblast adhesion and morphology in comparison with an anodized Ti6Al4V alloy and a non-anodized Ti6Al4V surface. These results suggest

that SOW could potentially be used as a disinfecting agent for nanostructured implant biomaterials without compromising their performance.

5. Disclosures

The authors declare no conflict of interest regarding the publication of this article.

Acknowledgments

This work was supported by the Consejo Nacional de Ciencia y Tecnología (CONACYT-CVU 348737, 114359), Mexico, for a PhD Scholarship. The authors also want to acknowledge to UABC due to the grant number 2058 from 1ra Convocatoria Especial Para PTC Contratados en 2013 y 2014.

References

[1] F. Ordikhani, A. Simchi, Appl. Surf. Sci. 317 (2014) 56–66.
[2] K.M. Kummer, E.N. Taylor, N.G. Durmas, K.M. Tarquinio, B. Ercan, T.J. Webster, J. Biomed. Mater. Res. B Appl. Biomater. 101 (2013) 677–688.
[3] A. Winkel, W. Dempwolf, E. Gellermann, M. Sluszniak, S. Grade, W. Heuer, M. Eisenburger, H. Menzel, M. Stiesch, Int. J. Mol. Sci. 16 (2015) 4327–4342.
[4] A.M. Gallardo-Moreno, M.A. Pacha-Olivenza, M.-C. Fernández-Calderón, C. Pérez-Giraldo, J.M. Bruque, M.-L. González-Martín, Biomaterials 31 (2010) 5159–5168.
[5] M.A. Arenas, C. Perez-Jorge, A. Conde, E. Matykina, J.M. Hernandez-Lopez, R. Perez-Tanoira, J.J. de Damborenea, E. Gomez-Barrena, J. Esteba, Colloids Surf. B Biointerfaces 105 (2013) 106–112.
[6] W.Q. Yu, X.Q. Jiang, L. Xu, Y.F. Zhao, F.Q. Zhang, X. Cao, J. Biomed. Mater. Res. B Appl. Biomater. 99 (2011) 207–216.
[7] S. Oh, C. Daraio, L.H. Chen, T.R. Pisanic, R.R. Finones, S. Jin, J. Biomed. Mater. Res. A 78 (2006) 97–103.
[8] K.S. Brammer, S. Oh, C.J. Cobb, L.M. Bjursten, H.v.d. Heyde, S. Jin, Acta Biomater. 5 (2009) 3215–3223.
[9] B. Ercan, E. Taylor, E. Alpaslan, T.J. Webster, Nanotechnology 22 (2011) 295102.
[10] C. Perez-Jorge, A. Conde, M.A. Arenas, R. Perez-Tanoira, E. Matykina, J.J. de Damborenea, E. Gomez-Barrena, J. Esteban, J. Biomed. Mater. Res. A 100 (2012) 1696–1705.
[11] E. Beltrán-Partida, B. Valdez-Salas, A. Escamilla, A. Moreno-Ulloa, L. Burtseva, E. Valdez-Salas, M. Curiel Alvarez, N. Nedev, J. Nanomater. 2015 (2015) 1–9.
[12] X.L. Liu, W.R. Zhou, Y.H. Wu, Y. Cheng, Y.F. Zheng, Mater. Sci. Eng. C 33 (2013) 4144–4154.
[13] L. Zhao, S. Mei, W. Wang, P.K. Chu, Z. Wu, Y. Zhang, Biomaterials 31 (2010) 2055–2063.
[14] S. Oh, K.S. Brammer, K.-S. Moon, J.-M. Bae, S. Jin, Mater. Sci. Eng. C 31 (2011) 873–879.
[15] M. Hirano, T. Kozuka, Y. Asano, Y. Kakuchi, H. Arai, N. Ohtsu, Appl. Surf. Sci. 311 (2014) 498–502.
[16] J.H. Park, R. Olivares-Navarrete, R.E. Baier, A.E. Meyer, R. Tannenbaum, B.D. Boyan, Z. Schwartz, Acta Biomater. 8 (2012) 1966–1975.
[17] C. Landa-Solis, D. Gonzalez-Espinosa, B. Guzman-Soriano, M. Snyder, G. Reyes-Teran, K. Torres, A.A. Gutierrez, J. Hosp. Infect. 61 (2005) 291–299.
[18] J. Medina-Tamayo, E. Sánchez-Miranda, H. Balleza-Tapia, X. Ambriz, M.E. Cid, D. González-Espinosa, A.A. Gutiérrez, C. González-Espinosa, Int. Immunopharmacol. 7 (2007) 1013–1024.
[19] S. Sekiya, K. Ohmori, K. Harii, Artif. Organs 21 (1997) 32–38.
[20] M.E. Velazquez-Meza, M. Hernandez-Salgado, M.A. Sanchez-Aleman, Microb. Drug Resist. (Larchmont, N.Y.) 21 (2015) 367–372.
[21] V. Zinkevich, I.B. Beech, R. Tapper, I. Bogdarina, J. Hosp. Infect. 46 (2000) 153–156.
[22] T.-Y. Chen, S.-H. Kuo, S.-T. Chen, D.-F. Hwang, Food Chem. 194 (2016) 529–537.
[23] R.M.S. Thorn, S.W.H. Lee, G.M. Robinson, J. Greenman, D.M. Reynolds, Eur. J. Clin. Microbiol. Infect. Dis. 31 (2012) 641–653.
[24] E. Beltrán-Partida, A. Moreno-Ulloa, B. Valdez-Salas, C. Velasquillo, M. Carrillo, A. Escamilla, E. Valdez, F. Villarreal, Materials 8 (2015) 867–883.
[25] C. Yao, E.B. Slamovich, T.J. Webster, J. Biomed. Mater. Res. A 85 (2008) 157–166.
[26] G. Lan, M. Li, Y. Tan, L. Li, X. Yang, L. Ma, Q. Yin, H. Xia, Y. Zhang, G. Tan, C. Ning, J. Mater. Sci. Technol. 31 (2015) 182–190.
[27] C.J. Frandsen, K.S. Brammer, K. Noh, G. Johnston, S. Jin, Mater. Sci. Eng. C 37 (2014) 332–341.
[28] G. Bjerkan, E. Witso, K. Bergh, Acta Orthop. 80 (2009) 245–250.
[29] I. Yoda, H. Koseki, M. Tomita, T. Shida, H. Horiuchi, H. Sakoda, M. Osaki, BMC Microbiol. 14 (2014) 234.
[30] B. Ercan, T.J. Webster, Int. J. Nanomedicine 3 (2008) 477–485.
[31] K. Burns, C. Yao, T.J. Webster, J. Biomed. Mater. Res. A 88 (2009) 561–568.
[32] B. Ercan, K.M. Kummer, K.M. Tarquinio, T.J. Webster, Acta Biomater. 7 (2011) 3003–3012.
[33] R. Olivares-Navarrete, S.E. Rodil, S.L. Hyzy, G.R. Dunn, A. Almaguer-Flores, Z. Schwartz, B.D. Boyan, Biomaterials 51 (2015) 69–79.
[34] W. Att, N. Hori, F. Iwasa, M. Yamada, T. Ueno, T. Ogawa, Biomaterials 30 (2009) 4268–4276.
[35] Y. Han, D. Chen, J. Sun, Y. Zhang, K. Xu, Acta Biomater. 4 (2008) 1518–1529.
[36] S. Faghihi, F. Azari, A.P. Zhilyaev, J.A. Szpunar, H. Vali, M. Tabrizian, Biomaterials 28 (2007) 3887–3895.
[37] J.A. Wilkins, S. Lin, Cell 28 (1982) 83–90.
[38] G. Daculsi, P. Pilet, M. Cottrel, G. Guicheux, J. Biomed. Mater. Res. 47 (1999) 228–233.
[39] J.W. Lee, K.B. Lee, H.S. Jeon, H.K. Park, Anal. Sci. Int. J. Jpn. Soc. Anal. Chem. 27 (2011) 369.
[40] S.D. Puckett, E. Taylor, T. Raimondo, T.J. Webster, Biomaterials 31 (2010) 706–713.
[41] W.T. Lin, H.L. Tan, Z.L. Duan, B. Yue, R. Ma, G. He, T.T. Tang, Int. J. Nanomedicine 9 (2014) 1215–1230.
[42] H. Zhang, Y. Sun, A. Tian, X.X. Xue, L. Wang, A. Alquhali, X. Bai, Int. J. Nanomedicine 8 (2013) 4379–4389.
[43] T.E. Cloete, M.S. Thantsha, M.R. Maluleke, R. Kirkpatrick, J. Appl. Microbiol. 107 (2009) 379–384.